AURORAL ELECTROJETS AND 3D CURRENTS IN THE IONOSPHERE-MAGNETOSPHERE SYSTEM

Y.I. Feldstein[1], V.A. Popov[1], J.A. Cumnock[2], A. Prigancova[3], L.G. Blomberg[2], J.U. Kozyra[4], B.T. Tsurutani[5], L.I. Gromova[1], A.E. Levitin[1]

[1]*Institute of Terrestrial Magnetism, Ionosphere and Radio Wave Propagation, Troitsk, Moscow Region, Russia*
[2]*Alfvén Laboratory, Royal Institute of Technology, Stockholm, Sweden*
[3]*Geophysical Institute, Slovak Academy of Sciences, Bratislava, Slovakia*
[4]*Space Physics Research Laboratory, University of Michigan, Ann Arbor, MI, USA*
[5]*Jet Propulsion Laboratory, Pasadena, CA, USA*

Abstract. There are shortly described results of the analysis of variations in the location and intensity of the auroral electrojets during magnetic storms and substorms using a numerical method for estimating the equivalent ionospheric currents based on data from meridian chains of magnetic observatories. It is shown that the westward electrojet adjoins to the polar electrojet located at cusp latitudes in the dayside sector. The association of electrojets with the field-aligned currents (FACs), namely Region 1 FAC and Region 2 FAC is considered. During intense disturbances a Region 3 FAC (accompanied with diffuse electron precipitation from the plasma sheet boundary layer) with the downward current was identified. The analysis of observational data is summarized in terms of 2D time-latitude distribution of electrojets at ionospheric altitudes. The magnetic field sawtooth variations generated during the storm main and early recovery phases are also discussed. To follow 3D currents in the magnetosphere-ionosphere system a clarified view of interrelated 3D currents and magnetospheric plasma domains is presented.

1. Introduction

The auroral electrojets (westward and eastward ones) had been identified at high latitudes earlier [Chapman, 1935]. During magnetospheric substorms and magnetic storms the westward electrojet (WE) is usually related to the morning sector, while the eastward electrojet (EE) is considered to be characteristic for the evening sector. The WE intensity is several times higher that of the EE. The magnetic effect of electrojets on the Earth's surface can be as high as 3000 nT.

The further progress in our understanding of the electrojet dynamics starts in the early sixties when the paradigm of the auroral zone was replaced with a new one of the auroral oval (AO) as stressed by Akasofu [2002]. Concurrently a new large-scale model of the equivalent ionosphere currents and their distribution at high latitudes was suggested [Feldstein, 1963; Akasofu et al., 1965; Feldstein and Zaitsev, 1965]. In this contribution the stormy interval of 24-25 September 1998 was analyzed using both ground-based observations (data from three magnetometer chains) and satellite measurements (data on particle precipitations and FAC) in order to study the electrojet dynamics, their relationship to field-aligned currents (FACs) and to plasma domains in the magnetosphere.

2. Interplanetary and geophysical conditions

The time interval of 24–25 September 1998 was selected for the analysis. It includes the GEM magnetic storm (on 25 September) and the preceding magnetospheric substorms (on 24 September). Space weather conditions can be followed using data on solar wind and IMF parameters on board of the ACE spacecraft (located at approximately X=241, Y= -18,

Z=27 R_E GSM). Fig. 1 shows 1-min averages of these parameters. The geophysical situation during the interval analyzed is characterized by the 1-min averages of geomagnetic indices Sym-H, AU, and AL (data from the Kyoto WDC).

On 24 September from 00 UT to 10 UT a few successive substorms were observed. After 15 UT B_z becomes a southward one. This leads to continuous prestorm geomagnetic activity. The enhanced geomagnetic activity was initiated by a fast forward
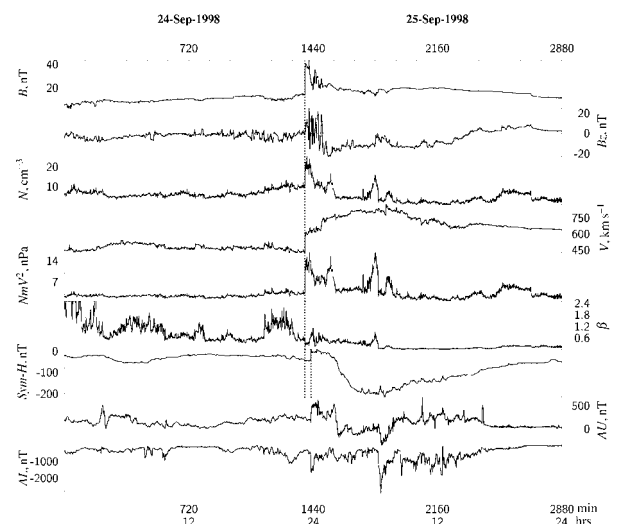

Fig. 1. ACE measurements (1-minute averages) of the IMF intensity B, north-south Bz component, solar wind plasma density N, solar wind velocity V, solar wind ram pressure P, and plasma β (the ratio of plasma and magnetic pressures). The last three profiles correspond to geomagnetic indices (1-minute averages) Sym-H, AU, and AL on 24–25 September 1998.

shock compression of the magnetosphere that was noted at ACE at 2312 UT on 24 September 1998 (the first vertical dotted line in Fig. 1). This is identified by the IMF magnitude increase from 15.2 to 40.5 nT, the density from 10.0 to 22.4 cm^{-3}, and the ram pressure jump from 3.4 nPa to 14.2 nPa at the shock. A large magnetic storm was initiated by sheath southward magnetic fields and extended by magnetic cloud with southward magnetic fields. At the time of shock impingement at ~23 47 UT there is a storm sudden commencement (SSC) when Sym-H increases from -44 nT to ~ 0 nT (the second vertical dotted line in Fig. 1). Hence there is a propagation delay of 35 min for the shock to arrive to the magnetosphere from ACE. The magnetic storm main phase begins at about 0115 UT on 25 September. The peak Sym-H value of **-**206 nT is reached at 0603 UT. There is a sharp interplanetary discontinuity that occurs at 06 15 UT. There are also a density, a ram pressure, and the plasma beta value (to less than 0.1) decreases at that time. The IMF magnitude of **~** 18.5 nT is smooth after this time. The low beta and high intensity**,** smooth magnetic fields identify the interval from 06 15 UT up to the end of 25 September as the magnetic cloud portion of the interplanetary coronal mass ejection [Burlaga et al, 2001] . According to the Sym-H index the maximum storm main phase depression lasts during 05-09 UT when the minimum value of Sym-H within a range of (–200, –217 nT) is reached. The recovery phase starts with a rapid recovery of Sym-H until 16 UT followed by a substantially slower recovery.

3. Modelling of equivalent ionospheric currents

A numerical method used to obtain intensity estimates of the equivalent ionospheric currents is based on data from meridional chains of magnetic observatories as described by Popov and Feldstein [1996], Popov et al [2001].

The inversion scheme to infer latitudinal fine structure of the auroral electrojet by utilizing series of narrow ionospheric current strips (100 altogether) of different intensities located at the 115 km altitude was used. Below, the refined method by Popov and Feldstein (1996) is applied to some substorms and a magnetic storm in September 1998 in order to obtain the location and distribution of auroral and polar electrojets intensities as a function of latitude. For this study, data from three meridian magnetometer chains (the IMAGE chain along the 110º CG longitude, the GWC chain along the 40º CG longitude, and the CANOPUS chain along the 330º CG longitude) covering a wide range of corrected geomagnetic latitudes Φ were used. In Fig.2 H component measurements from the IMAGE chain on 25 September 1998 can be seen as an example of Φ vs UT plots of the eastward and westward currents density (top panel) and their total intensities (bottom panel). Similar plots (not shown) were obtained for 24 and 25 September 1998 using data on H and Z variations from three chains of observatories separately (visit http://pgi.kolasc.net.ru/seminar/ to see Fig. 2 in color).

The results of the analysis give evidence of the dynamics of electrojet during substrom and storm conditions.

During substorms the characteristics of the eastward/westward currents can be summarized as follows:
° westward currents are most intense around midnight hours at auroral latitudes of $65° < \Phi < 70°$, and are shifted to cusp latitudes ($\Phi \sim 77°$) in the morning and evening sectors;
° eastward currents in the evening sector shift from cusp latitudes ($\Phi \sim 77°$) during the early afternoon MLT hours, reach the auroral latitudes by night hours and become more intense in the evening MLT;
° eastward currents are located just equatorward of the westward currents for evening hours where currents in opposite directions overlap in latitude.

The enhancement of the ring current intensity (Sym-H index in Fig. 1) during 00-04 UT is accompanied by intense westward currents seen by the IMAGE chain (Fig.2) during night time and early morning MLT hours.
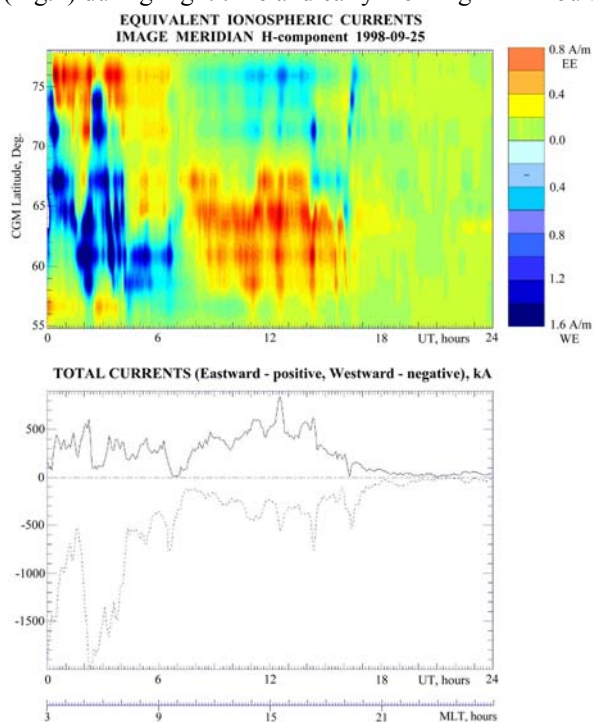

Fig. 2. The corrected geomagnetic latitude vs UT plot of the eastward and westward equivalent ionospheric currents as calculated using H component data on 25 September 1998 from the IMAGE meridian chain of magnetic observatories (top panel). Total intensity of the eastward and westward currents according to the IMAGE chain H component (bottom panel). See also Fig. 2 in color on the web.

During the substorm these currents cover the latitudinal range from $\Phi \sim 75°$ to $\sim 58°$. Under these conditions the eastward equivalent currents do not disappear. Rather, they persist in the near midnight-morning sector but are shifted to subauroral latitudes, $\Phi < 57°$. The latitudinal range of westward currents (as seen by the IMAGE chain) becomes narrower (about ~5°) by morning and

before noon hours. According to the IMAGE magnetic data the eastward current that can be identified as PE, appears at Φ ~66°–68° after 08 UT (11 MLT) and is
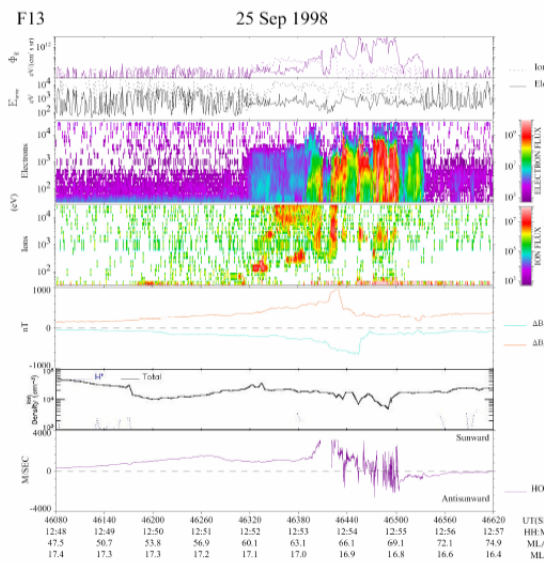

Fig. 3. Plasma measurements within the 1248–1257 UT interval on 25 September 1998 during the DMSP F13 pass over auroral latitudes. From top to bottom: energy flow and mean energy of electrons and ions (first and second panels); energy spectrograms of electrons and ions (third and fourth panels); variations of the magnetic field eastwest (Bz, brown) and north-south (By, green) components (fifth panel); ion density (sixth panel); plasma drift velocity (seventh panel).

located in the cusp (CU) region. Actually, according to the DMSP F11, F12, and F14 particles data the CU shifts to Φ ~ 65°–67° during 08–15 UT, i.e., during the storm main phase and the beginning of the storm recovery phase. The positive IMF By during this time interval is another indication that the eastward current is the PE. The weak westward currents poleward of the PE are a consequence of the magnetic field disturbances in the polar cap (PC) due to the FAC.

Equatorward of the PE the EE is found as a wide strip directly adjoining the CU. Eastward current can cover latitudes up to Φ~58°. Its variations in intensity and latitude are sawtooth-like. Sawtooth oscillations of energetic proton/electron fluxes measured by geostationary spacecraft during magnetic storm intervals are currently of immense interest to the scientific community. These oscillations and the accompanied geophysical phenomena as well as their correlation with interplanetary parameters were recently analyzed in a number of studies. Summarizing the results obtained it can be stated that conclusions on the relationship between solar wind parameters and sawtooth oscillations are contradictory: the sawtooth oscillations are directly driven by the series of solar wind pressure enhancements and are not the result of an internal magnetospheric process, e.g. of a substorm [Lee et al, 2004]; the sawtooth-like flux oscillations represent

periodic substorms and the period of the substorms is determined by the magnetosphere rather than by the solar wind [Huang et al, 2005]. Nevertheless the investigation of the auroral electrojet behaviour within the intervals of sawtooth oscillations was out of the scope of these two and other investigations. It appears to be reasonable to consider the peculiarities of auroral electrojets during the 25 September magnetic storm, when sawtooth oscillations occur. It is worth stressing that this storm was analyzed by both teams mentioned above. If sawtooth oscillations are periodically repeated substorms, then evidence of their typical features and consequently the characteristic auroral electrojet features can be expected to be necessary signatures of sawtooth oscillations. Such features are shortly summarized below:

1. As seen in Fig. 2, the EE bursts on the IMAGE meridian occur at 08–16 UT. These bursts occur within the latitudinal range 58° < Φ < 66°. The distinctive peaks in the total intensity profile of eastward currents are indications of the occurrence of bursts (Fig. 2, bottom panel).

2. The beginnings and maxima (in brackets) of the EE bursts in UT are 0830 (0850); 1000 (1130); 1150 (1230); 1320 (1420); 1520 (1540) and timing is in accord with sawtooth oscillations of plasma flaxes measured at geostationary orbits. The mean duration of individual bursts from their beginning to the maximum is within the range (20 min to an hour), spacing being of ~1.5–2.0 hours.

3. EE bursts on the IMAGE meridian in the evening sector are in accord with the occurrence of more intense WE on the CANOPUS meridian in the early morning sector. The time accordance between individual bursts in EE and WE intensity was not revealed.

4. The burst maximum on the IMAGE meridian precedes that on the GWC meridian by 20-30 min. The comparison of bursts along the IMAGE and GWC meridians during 11–16 UT showed that on the IMAGE meridian the intensity of bursts is ~300 kA whereas that on the GWC meridian is ~150 kA. It is likely that the two-fold decrease of the current intensity in the burst characterizes the scale of the burst current system. Such estimates show that the amplitude of sawtooth-like magnetic oscillations decreases twofold in the longitudinal range of ~60°.

5. Besides the first EE burst at 0830–0850 UT, the EE burst intensity (Fig. 2) is not unanimously associated with the solar wind pressure value (Fig. 1) when the time delay is taken into account. This task was already discussed in detail [Huang et al., 2005].

To summarize it can be stated that the peculiarities of the auroral electrojet behaviour during the 25 September 1998 main and recovery phases of the magnetic storm give evidence allowing to consider their sawtooth-like magnetic oscillations as realistic signature of magnetospheric substorms. In Fig.3 (shown at http://pgi.kolasc.net.ru/seminar/ only) the processed DMSP F13 observations for its pass over the auroral region on 25 September 1998 at 1248–1257 UT (~ 17

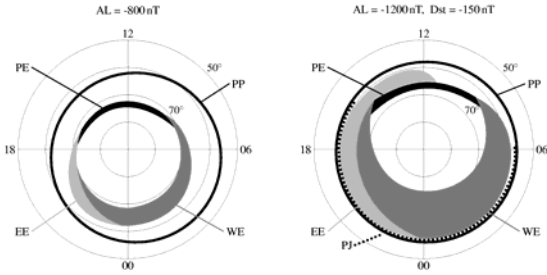MLT , i.e. nearby the IMAGE meridian, but somewhat later MLT) can be seen. The pass was related to the

Fig. 4. Schematic view of the space-time distribution of electrojets at ionospheric altitudes. Substorm and storm conditions are considered separately: the magnetospheric substorm with AL ~ –800 nT (left) and the magnetic storm main phase with AL ~ –1200 nT, Dst ~ –150 nT (right)**.** The location of the plasmapause (PP) and polarization jet (PJ) is also shown. See Fig. 4d,e in color on the web.

early recovery of the intense sawtooth activity. The spectrograms for electrons give evidence on three regimes of plasma precipitations, namely structured ones at auroral oval latitudes and diffuse precipitations equatorward and poleward of the auroral oval. The high-latitude boundary of the auroral plasma precipitation region (Fig. 3 on the web) is located at $\Phi=70.5°$. The currents in the high-latitude ionosphere are associated with the increase of its conductivity during auroral precipitations. Hence, westward equivalent currents at $\Phi>70.5°$ (Fig. 2) are not currents in the ionosphere, but are associated with the magnetic field variations due to magnetospheric sources.

In the region of the diffuse poleward precipitation the ionospheric plasma convection is antisunward and the one equatorward of this region is sunward. The field-aligned current inflows to ionospheric latitudes (Region 2 FAC) at diffuse precipitation latitudes for electrons and high-energy ions; at higher latitudes the current outflows from the ionosphere (Region 1 FAC). The EE latitudinal width of $58°< \Phi <66°$ (Fig. 2) is identical with the Region 2 FAC location. This FAC intensity can be determined using magnetic field variations data (see Fig. 3). If the field-aligned current is assumed to flow on an infinite 2D plane surface oriented east-west and the magnetic field variations measured by DMSP are caused by FAC only, then the current density $j_{\parallel}$ can be determined from the relationship $\dfrac{d\Delta Bz}{dx} = \mu_0\, j_{//}$, where $\mu_0 = 4\pi \times 10^{-7}$ H/m is the magnetic permeability in vacuum. In Region 2 FAC the mean current density and linear FAC density are $j_{//} \sim 0.64\mu A/m^2$ and $J_{//} \sim 0.5 A/m$, respectively. The $J_{//}$ value is lower than that of the linear ionospheric equivalent current density, $J_{ion} \sim 0.8 A/m$, within the interval of the DMSP F13 pass. The EE prolongation (in terms of MLT) is 8 hours (see Fig. 2) and the current inflowing into the ionosphere is ~ 3.7 MA.

During the main phase of the intense magnetic storm the following characteristics of the electrojet dynamics are apparent:

° during evening hours both the EE and WE shift equatorward; around late evening-midnight hours the EE is located at subauroral latitudes;

° the eastward and westward current intensities in the evening sector imply that the EE cannot be the consequence of the WE closing through lower latitudes;

° at the peak of the storm main phase and early recovery phase the equatorward boundary of the CU (and hence the PE) shifts to $\Phi\sim 65\text{-}67°$;

° at the main phase maximum the EE during near-noon hours adjoins the CU at $\Phi\sim65°$;

° the WE is absent in the day-time sector;

° when passing from midnight to morning hours the latitudinal width of the WE decreases, and the current shifts to higher latitudes.

4. Presentation of electrojets by the 2D equivalent ionospheric current and 3D current systems

An equivalent ionospheric current system is usually used for a generalized presentation of the distribution of perturbed geomagnetic field vectors on the Earth's surface. The widely known presentations (Fig. 4a,b,c at web mentioned) are the two-vortex classical current system (Fukushima, 1953), the single-vortex system with a WE along the auroral oval and closure currents through the PC and middle latitudes reported by Feldstein (1963) and Akasofu et al. (1965), and the two-vortex system with a WE within the boundaries of the auroral oval and with an EE in the evening sector at $\Phi \sim65°$(Feldstein and Zaitsev, 1965). It was concluded that during substorms the WE extends to all longitudes along the auroral oval and its intensity decreases from midnight to noon hours. The EE as a separate current system, rather than a return current from the WE, is located at $\Phi \sim65°$ in the evening sector.

The modification of these patterns based on our results is considered below for substorm and storm intervals (see also the colour presentation in Fig. 4d,e at web mentioned). The space-time distribution of currents (ionospheric altitudes) and their structure at high latitudes during the magnetospheric substorm with the intensity of AL ~ –800 nT is shown in Fig. 4 (left).

The location of the WE can be easily seen. Its latitudinal width is ~6° during midnight-dawn hours. During evening and pre-noon hours the WE extends from lower latitudes to the CU. As seen in Fig. 4 (left) the WE does not cover all MLT hours (contrary to earlier results, e.g. Figs 4b,c) during the substorm, but is seen only in the evening-night-morning hours. During the before-noon and after-noon hours the WE adjoins the CU, i.e. is magnetically mapped to the magnetopause. The narrow strip (2°–3° along the latitude) of the PE is located at the latitudes of the

ionospheric projection of the CU. The direction and current intensity in the PE is controlled by the IMF By component. It is likely that the WE continuity over all longitudes (Feldstein, 1963; Akasofu et al., 1965) was obtained since most of the data used were related to IMF By < 0 nT. As a result the WE and PE currents could not be distinguished and only one current strip was reported. In addition, during substorms the location of the most intense ionospheric currents is significantly asymmetric with regard to the noon-midnight meridian. In the noon sector the currents are located more poleward (~8°) than in the midnight sector.

The EE comprises the evening sector from early evening to midnight hours and is located at lower latitudes closer to midnight. Both the EE width and its intensity reach the maximum during dusk hours. The EE shown in Fig. 4 (left) is not a closure current for the WE at higher latitudes (contrary to earlier results, e.g. Fig. 4b) and is not located (contrary to earlier results, e.g. Fig. 4**c**) in the auroral zone (Φ ~65°)**.** According to Fig. 4 (left) the EE latitude increases from night to evening hours. During early evening hours the EE adjoins the ionospheric projection of the CU, i.e. the EE is magnetically mapped to the magnetopause during this MLT interval.

In Fig. 4 (right) the distribution of equivalent currents and their structure during the storm main phase with activity indices of AL ~ −1200 nT and Dst = −150 nT are shown. The intensity of the electrojets increases. They are shifted to lower latitudes in comparison to substorm conditions (Fig**.** 4, left). The westward current during the morning hours can be seen starting from Φ ~57° within a latitudinal interval of ~15°. At the late morning and early evening hours the westward currents adjoin the PE. The PE during day hours is shifted equatorward to Φ~67° and the width of its narrow strip is 2°–3°. The WE asymmetry with regard to the noon-midnight meridian is valid for storm intervals (similarly to the substorm intervals). However, the asymmetry pattern changes essentially, in the night sector the WE poleward boundary is located at higher latitudes than the PE in the noon sector.
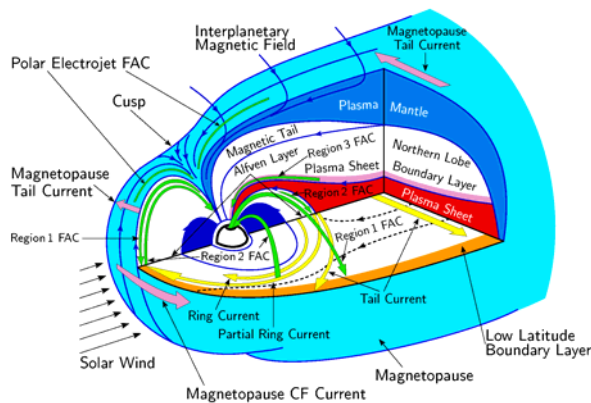
The EE envelops the WE along its equatorward boundary during not only evening-early dawn hours. The EE exists at latitudes between the PE and plasmapause up to noon during the main phase of the intense storm. At this time the bursts of the ion drift velocity of as much as ~4 km/s (SAPS – subauroral polarization stream) occur at subauroral latitudes (outside of the plasmapause) in the region of the ionospheric trough. In Fig. 4 (right) the location of the SAPS is indicated by a dotted line, the longitudinal prolongation of which is adopted from Foster and Vo (2002).

The structure of magnetospheric plasma domains and the 3D current systems is displayed in Fig. 5 (see also the colour presentation at web). The magnetosphere is shown in the meridian midday-midnight and equatorial planes, using ground-based observations of different types of auroral luminescence and auroral precipitation (Galperin and Feldstein, 1991). The majority of plasma domains seen in the figure are directly related to large-scale current systems in the magnetosphere.

The large-scale structure of plasma domains and its association with the occurrence of different geophysical phenomena in the upper atmosphere at high latitudes and on the Earth's surface were discussed in detail by Paschmann et al. [2003 and references therein], Galperin and Feldstein [1996 and references therein].

The 3D structure of currents in the near-Earth space is enclosed by the magnetopause. The currents screening magnetic fields in the inner magnetosphere from penetrating into the solar wind are located on the magnetopause. These eastward Chapman-Ferraro (CF) currents screen the dipole field. The magnetopause screening currents for the ring current (RC) fields are in the same direction, but their intensity is an order of magnitude weaker. The tail current (TC) in the CPS is in the dawn-dusk direction. The closure of the TC is attributed to currents on the magnetopause which exist not only on the night side, as well established, but on the day side as well. In Fig. 5 the TC in the equatorial plane of the magnetosphere is indicated by two vectors. At midnight one of them is located in the innermost part of the current sheet, the other along its boundary. The first remains in the tail and the second reaches the day side of the magnetopause where the directions of the CF and TC are opposite as seen in Fig. 5. Since CF currents are always more intense than TC closure currents the resulting current on the day side is always eastward oriented.

The FAC flowing into and out of the ionosphere in the vicinity of the PE are located on the CU surface. In Fig. 5 PE FAC are indicated with two green lines (not vectors) along the magnetic field. The PE FAC direction is not shown since it is controlled by the IMF By component: under By > 0 nT (By < 0 nT) the current flows into (out of) the ionosphere along the cusp inner surface and out of (into) it along its outer surface. The ionospheric closure of the inflowing and outflowing PE FAC is by Pedersen current.

Fig. 5. The 3D system of electric currents in the magnetosphere during a magnetic storm. See also Fig. 5 in color on the web.

The Region 1 FAC in the dusk sector is usually believed to be mapped magnetically from the ionosphere to the LLBL, i.e. to the vicinity of the magnetospheric boundary with the solar wind. Such a pattern is valid for Region 1 FAC during day-time hours only and is shown with a current arrow, resting against the LLBL. During the dusk and before midnight hours, where Region 1 FAC is located at auroral oval latitudes, FACs inflow to the CPS, i.e., into the deep magnetosphere. The Region 2 FAC flows into the ionosphere from the Alfvén layer periphery where the PRC is located. In Fig. 5 Region 2 FACs are indicated by three vectors for day, dusk and night hours. It is generally believed that the Region 2 FAC is located in the inner magnetosphere and is a part of the single current system with the EE and PRC. In the early afternoon sector, where the EE adjoins the PE, the Region 2 FAC in the equatorial plane of the magnetosphere is near the LLBL.

The RC and PRC are formed by westward drifting (around the Earth) energetic ions. In the RC region ions circulate many times around the Earth. In the PRC region the drift is interrupted before a full rotation and the ions depart from the magnetosphere, either precipitating into the ionosphere or reaching the magnetopause around noon. To fulfil the requirement for the PRC-Region 2 FAC-EE current system closure a field-aligned current from the ionosphere into the magnetosphere at about midnight hours is needed. Such a current exists at near-midnight hours and is shown by the vector in Fig.5.

A characteristic morphological feature of auroral electrojets exists in the evening sector, namely their overlapping. This is due to the additional Region 3 FAC current flowing into the ionosphere from the plasma sheet boundary layer (Fig.5) during intense magnetic disturbances. A southward electric field, favourable for the appearance of westward ionospheric Hall currents near the PC boundary, appears between the Region 3 FAC and Region 1 FAC. As a result the spatial overlapping of electrojets takes place.

The current wedge in the night-time sector of auroral latitudes is not shown in Fig.5.

References

Akasofu, S.-I.: Exploring the secrets of the aurora, Dordrecht, Kluwer Academic Publ., 2002, 235 p.

Akasofu, S.-I, Chapman, S., and Meng, C.-I.: The polar electrojet, J. Atmos. Terr. Phys., 27, 1275–1305, 1965.

Burlaga, L.F., Skoug, R.M., Smith, C.W., Webb, D.F.,Zurbuchen, T.H., and Reinard, Alysha, Fast ejecta during the ascending phase of solar cycle 23: ACE observations,1998-1999, J. Geophys. Res., 106, 20957–20977, 2001.

Feldstein, Y.I.: The morphology of aurora and geomagnetism, Aurora and Airglow, The Academy of Sciences of the U.S.S.R., N 10, 121–126, 1963 (in Russian).

Feldstein, Y.I., and Zaitzev, A.N.: The current system of SD-variations in high latitudes for the winter season during the IGY, Geomag. and Aeronomie, 5, N6, 1123–1128, 1965.

Foster, J.C., and Vo, H.B.: Average characteristics and activity dependence of the subauroral polarization stream, J. Geophys, Res., 107, A12, 1475, doi: 10.1029/2002JA009409, 2002.

Fukushima, N.: Polar magnetic storms and geomagnetic bays, J. Fac. Sci., Tokyo Univ., 8, part 5, 293–412, 1953.

Galperin, Yu.I, and Feldstein, Y.I.: Auroral luminosity and its relationship to magnetospharic plasma domains, in Auroral Physics, ed. by C.-I. Meng, M.J. Rycroft, and L.A. Frank, Cambridge UP, 207–222, 1991.

Galperin, Yu.I, and Feldstein, Y.I.: Mapping of the precipitation region to the plasma sheet, J. Geomag. Geoelectr., 48, 857–875, 1996.

Huang, C.-S., Reeves, G.D., Le, G., and Yumoto, K., Are sawtooth oscillations of energetic plasma particle fluxes caused by periodic substorms or driven by solar wind pressure enhancements? J. Geophys, Res., 110, A07207, doi: 10.1029/2005JA011018, 2005.

Lee, D.-Y., Lyons, L.,R., and Yumoto, K., Sawtooth oscillations directly driven by solar wind dynamic pressure enhancements,J. Geophys, Res., 109, A04202, doi: 10.1029/2003JA010246, 2004.

Paschmann, G., Haaland, S., and Treumann, R.(eds.), Auroral plasma physics, Dordrecht, Kluwer Academic Publishers, The Netherlands, 485 p., 2003.

Popov, V.A., and Feldstein, Y.I., About a new interpretation of "Harang discontinuity", Geomagn.Aeron., 36(1), 43-51, 1996.

Popov, V.A., Papitashvili, V.O., and Watermann, J.F., Modeling of equivalent ionospheric currents from meridian magnetometer chain data, Earth Planets Space, 53, 129-137, 2001.